# Possible use of rotational ground motions in oilfield studies:

# Part I: Theory, Observations, Processing

**H. Igel, N.D. Pham, M. Bernauer, A. Fichtner, M. Käser, J. Wassermann**
**Department of Earth Sciences, LMU Munich**

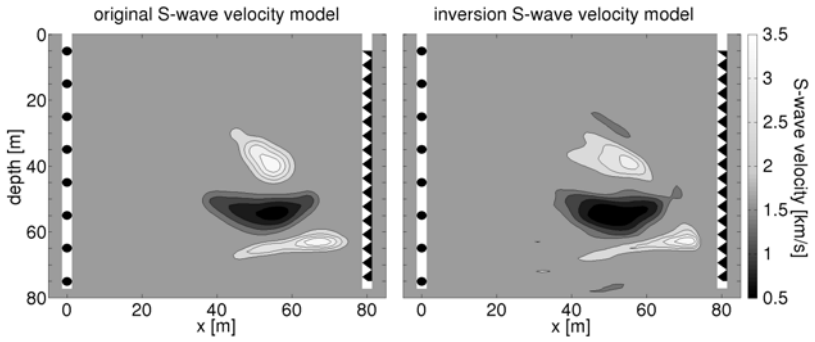


**This is a report under a *Confidential Information Disclosure Agreement* between the Ludwig-Maximilians-University, Munich, and Schlumberger K.K., Japan.**

# Table of Contents

## Abstract

With the recent advent of instruments (e.g., ring laser, fluid-based sensors, fiber-optic gyros) that allow accurate observations of rotational ground motions and the first consistent comparisons with translations, research into the theory and application of rotational motions is rapidly growing (see special issue of the Bulletin of the Seismological Society of America in May 2009). Within the theory of linear elasticity ground rotations occur for shear waves inside the medium and all other wave types at the free surface. It can be shown that point measurements of both rotations and translations allow the extraction of wavefield features (e.g., direction of propagation, apparent phase velocities) that otherwise are only recoverable from seismic arrays. Ground rotations are relevant and/or useful for (1) correcting translational measurements for cross-coupling effects; (2) structural and/or source inversion; (3) recovery of scattering properties; (4) separating shear and P-wave energy. Here we present recent discoveries particularly in the area of inversion and broadband data processing focusing on aspects that might be relevant for reservoir problems.

## 1. Introduction: Why measuring rotations?

Currently there are two types of measurements that are routinely used to monitor seismic wave fields. Standard inertial seismometers measure three components of translational ground displacement (velocity, acceleration) and form the basis for monitoring seismic activity and carrying out active and passive seismic experiments to recover Earth's structure. The second type aims at measuring the deformation of the Earth (strains). It has been noted for decades (Aki and Richards, 2002, and previous edition) that there is a third type of measurement that is needed in seismology and geodesy in order to fully describe the motion at a given point, namely the measurement of ground rotation. The three components of seismically induced rotation have been extremely difficult to measure, primarily because previous devices did not provide the required sensitivity to observe rotations in a wide frequency band and distance range (the two horizontal components, equal to tilt at the free surface, are generally recorded at low frequencies, but are contaminated by translations). It is important to note that – particularly in the near field – seismic inertial sensors are contaminated by rotations, one of the main reasons why it is so difficult to integrate strong motion recordings to displacements (e.g., Trifunac and Todorovska, 2001; Graizer, 2005, 2006).

Following the pioneering observations with ring laser rotation sensors in Christchurch, New Zealand (McLeod et al., 1998; Pancha et al., 2000) a ring laser built for the observations of the Earth's rotation rate located at Wettzell, Germany (Schreiber et al., 2006, 2009) was adapted to the sampling rate requirements in seismology allowing the observations of earthquake-induced rotational ground motions over a wide magnitude and epicentral distance range (Igel et al., 2005, 2007, Cochard et al., 2006). Analysis of these observations in combination with collocated recordings by a standard broadband seismometer showed the possibility of extracting additional information on subsurface structure compared to translational measurements alone (e.g., Suryanto, 2007; Pham et al., 2009; Ferreira and Igel, 2009; Fichtner and Igel, 2009, Bernauer et al., 2009), otherwise accessible with seismic array measurements only.

In the sections below we briefly review the state of the art of theory, observations and analysis of collocated measurements of rotations and translations and discuss potential applications to reservoir problems. Most of the presented results are parts of publications in print in the special

issue on “Rotational seismology” of the Bulletin of the Seismological Society of America to appear in the May issue of 2009.

Part I of the report is structured as follows: **Section 2** focuses on observations of rotations in terms of expected amplitudes in the context of reservoir-type micro-seismicity as well as our experience with current rotation sensor technology. We also discuss the first comparative studies of array-derived rotations vs. directly measured rotations. In **Section 3** we demonstrate the possibilities to process collocated observations of translations and rotations with examples of ring laser recordings and the R1 sensor. In **Section 4**, we present a recently developed theory applying adjoint techniques to a new observable based on joint observations of rotations and translations (called *apparent shear-wave speed*). Sensitivities with respect to Earth structure are calculated and a new tomographic scheme is developed and tested with synthetic examples. Finally in **Section 5**, we discuss the potential of these recent developments for oilfield applications. Some statements particularly relevant for potential applications are put in **bold** throughout the text.

Note that – in order to keep the part I concise and readable – only the fundamental concepts are introduced. Details on theory, processing, etc. as well as high-resolution figures can be found in the attached literature or in part II (processing of synthetic seismograms).

## 2. Observations of rotational motions

### *a. Expected rotational motion amplitudes (microseismicity)*

It is straight forward – at least assuming a homogeneous isotropic material – to estimate the expected amplitudes of rotation (rates) for a given source time function and scalar moment. The expression of the displacement u(x) generated by a point double-couple source in an infinite, homogeneous, isotropic medium for far field case is given by Aki and Richards, 2002 (equations 4.32 and 4.33, page 79):

$$\mathbf{u}(\mathbf{x},t) = \frac{1}{4\pi\rho\alpha^3}\mathbf{A}^{FP}\frac{1}{r}\dot{M}_0(t-\frac{r}{\alpha}) + \frac{1}{4\pi\rho\beta^3}\mathbf{A}^{FS}\frac{1}{r}\dot{M}_0(t-\frac{r}{\beta}) \qquad (1)$$

in which the far field P and S have radiation patterns are given, respectively, by

$$\mathbf{A}^{FP} = \sin 2\theta\cos\phi\hat{\mathbf{r}} \qquad (2)$$

$$\mathbf{A}^{FS} = \cos 2\theta\cos\phi\hat{\boldsymbol{\theta}} - \cos\theta\sin\phi\hat{\boldsymbol{\phi}} \qquad (3)$$

The corresponding rotations (including near- and intermediate-field terms) were derived by Cochard et al., 2006 (equations 30.3 and 30.4, page 395)

$$\boldsymbol{\omega}(\mathbf{x},t) = \frac{-\mathbf{A}^R}{8\pi\rho}\left[\frac{3}{\beta^3 r^3}M_0(t-\frac{r}{\beta}) + \frac{3}{\beta^3 r^2}\dot{M}_0(t-\frac{r}{\beta}) + \frac{1}{\beta^4 r}\ddot{M}_0(t-\frac{r}{\beta})\right] \qquad (5)$$

where

$$\mathbf{A}^R = \cos\theta\sin\phi\hat{\boldsymbol{\theta}} - \cos\phi\cos 2\theta\hat{\boldsymbol{\phi}} \qquad (6)$$

Some interesting conclusions can be drawn from this simple result: (1) In infinite homogeneous media there do exist near- and intermediate field parts, but they all arrive with shear-wave speeds; (2) each double-couple source with an earthquake-type slip source-time function leads

to a permanent rotation (near-field term proportional to $M_0(t)$ as in the case of translations). (3) The far-field waveform of rotation is proportional to the second derivative of the source time function (and thus contains higher frequencies than displacements).

The time dependent seismic moment rate can be defined by

$$\dot{M}_0(t) = M_0 \dot{s}(t) \qquad (7)$$

where the source time function rate $\dot{s}(t)$ of period *T* is a Gaussian function

$$\dot{s}(t) = \exp\left[-\left(\frac{\pi t}{T}\right)^2\right] \qquad (8)$$

and $M_0$ is the scalar seismic moment and that can be empirically related to magnitude $M_w$

$$M_0 = 10^{(1.5M_w + 9.05)} \text{ (Nm).} \qquad (9)$$

Considering micro-seismic events of magnitude $M_w$ between -4 and 0, frequencies from 5 Hz to 150 Hz, and epicentral distance D from 200m to 1000m, both translational and rotational motions can be calculated by using the aforementioned equations. The peak translational velocity and rotation rate can be calculated by taking the time derivative of (1) and (5).

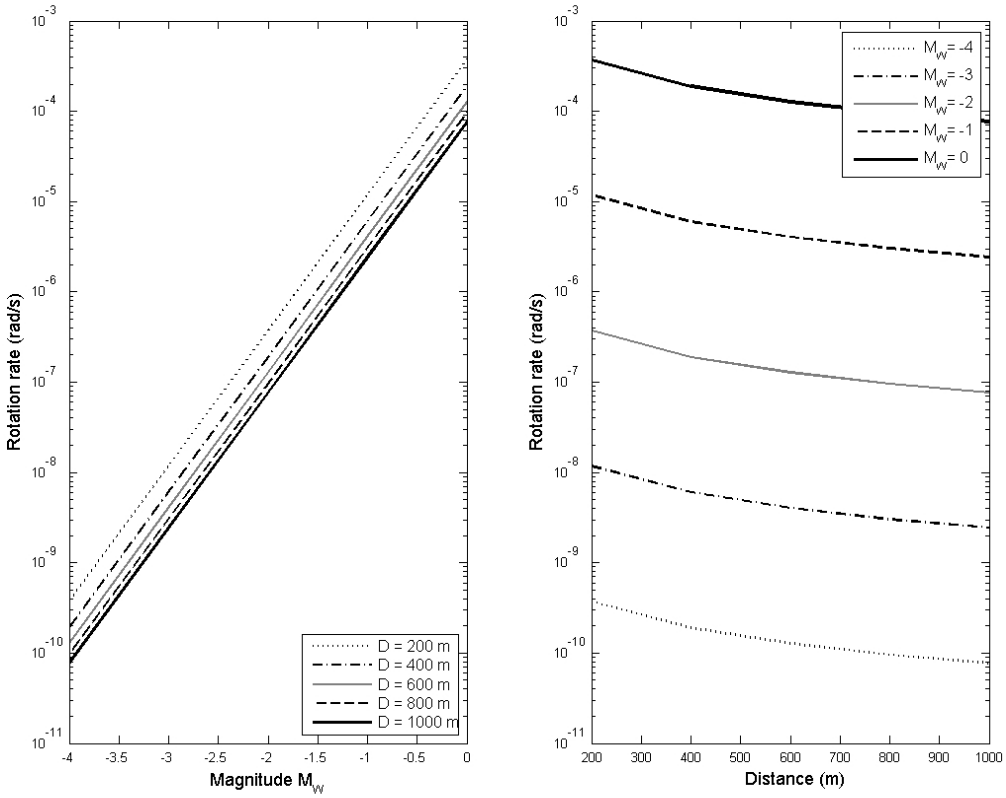


**Figure 1.** Peak rotation rate predicted for a dominant frequency *f* = 150 Hz as a function of magnitude and hypocentral distance.

For each set of magnitude $M_w$, distance D, and period T (or frequency), assuming P and S wave velocities to be $\alpha$ = 3800 m/s, $\beta$ = 2000 m/s, mass density $\rho$ = 2300 kg/m$^3$, we calculate

the peak values of translational velocity and rotation rate for all range of $\theta$, $\phi$, and time. Results for a source time function with a dominant frequency of 150 Hz are shown for rotation rate (the parameter measured by rotation sensors) in Figure 1 (all other results in Appendix A).

**At least for the parameter range considered one can immediately conclude that a (borehole) rotation sensor should be able to resolve rotation rates as small as $10^{-7}$ rad/s (100 nrad/s).** At a dominant frequency range of 150 Hz this would allow measuring wavefields up to a distance of approx. 1km down to magnitudes -2. The only available commercial rotation sensor R1 (www.eentec.com, see below) is reported to have a resolution of $1.2 \times 10^{-7}$ rad/s and in field tests rotation rates around 10 μrad/s could be recorded with sufficient signal-to-noise ratio (Wassermann et al., 2009). It is considered one of the biggest challenges to develop an appropriate (borehole) sensor that accurately and reliably measures rotations with similar quality than seismometers measure translations and with the required sensitivity to cover a wide range of applications.

### *b. Laser technology: Earth's rotation, seismic waves, borehole instrument orientation*

Even though not of interest for applications in reservoir-type applications in their present form we briefly review ring laser technology as most of the data presented here were recorded with such a system. In addition, optical approaches (e.g., fiber-optical gyros or small-scale ring lasers) are promising technologies for sensors in seismics and seismology.

Ring lasers detect the Sagnac beat frequency of two counter-propagating laser beams (see Schreiber et al., 2006, 2009 for a detailed description). These active interferometers are realised by triangular or (in our case) square closed cavities in which the light beams interfere. If this instrument is rotating on a platform with respect to inertial space, the effective cavity length between co-rotating and counter-rotating laser cavity differs and one obtains a frequency splitting (and thus a beating pattern) of the resulting standing wave. This beat frequency $\delta f$ is directly proportional to the rotation rate $\Omega$ around the surface normal **n** of the ring laser system as given by the Sagnac equation

$$\delta f = \frac{4A}{\lambda P}\mathbf{n}\cdot\boldsymbol{\Omega} \qquad (10)$$

where P is the perimeter of the instrument, A the area, and $\lambda$ the laser wavelength. This equation has three contributions that influence the beat frequency $\delta f$ : (1) Variations of the scale factor ($4A/\lambda P$) have to be avoided by making the instrument mechanically as rigid and stable as possible; (2) changes in orientation **n** enter the beat frequency via the inner product; and (3) variations in $\boldsymbol{\Omega}$ (e.g., due to changes in Earth's rotation rate, or seismically induced rotations) are representing the most dominant contribution to $\delta f$. Note that translations do not generate a contribution to the Sagnac frequency.

Ring lasers are sensitive to rotations only, given stable ring geometry and lasing. The second effect implies that for co-seismic observations at the Earth's surface the horizontal components of rotation (i.e., tilt) will contribute to the vertical component of rotation rate. As recently shown by Pham et al. (2009a) the tilt-coupling effect is several orders of magnitude below the level of the actual rotational signal unless one is very close to the source (ring lasers would not be the right technology).

A purpose-built ring laser system for seismology (Schreiber et al., 2009) was installed at the Pinon Flat Observatory, California, (PFO) in a dedicated underground chamber in 2005. Despite the sensitivity of the optical recording technology to external influences (temperature,

pressure variations) and resulting operational effects such as mode-hopping, the sensor has recorded several earthquakes (Schreiber et al., 2009).

Laser-based gyroscopes have been in use for some time in borehole seismic instruments (e.g., the borehole seismometer developed by Lennartz (www.lennartz-electronic.de). These low-resolution gyroscopes are used to determine the orientation of the borehole instrument by integrating the recorded rotation rates. It is not clear whether this technology can be further developed to be of interest to downhole recordings of rotational motions in seismic wavefields.

### *c. The R1 sensor*

To our knowledge there is currently only one commercially available rotation sensor with a sensitivity sufficient for seismic purposes. The sensor is called R1 (http://www.eentec.com/R-1_data_new.htm), developed by the company *eentec*. The sensor is based on electro-chemical effects and contains a liquid that moves in case of rotational motions. The BSSA special issue to be published in May 2009 contains several papers by Taiwanese and other groups reporting observations with the R1 sensor (e.g., Nigbor et al., 2009; Liu et al., 2009; Lin et al., 2009; Lee et al., 2009). Most of these papers merely present observations but no comparison with translations or a comparison with array-derived rotations.

In our view one of the options to test the accuracy of such sensors is to compare with array-derived rotations (principle described in the section below). In 2008 we recorded the collapse of a building with a small seismic array around the R1. Despite the fact that the experiment suffered from quite heterogeneous instruments (broadband and various short period sensors), the conclusions concerning the R1 sensor were encouraging (see Figure 2, and Wassermann et al., 2009, for details):

- The comparison between array-derived rotation and R1 recorded rotation showed good agreement concerning the peak rotation-rate amplitudes on all three components
- The waveform comparison between the z-component of rotation (array-derived vs. R1) in a narrow frequency band (1-8Hz) is surprisingly good. The fit is substantially worse for the other two components (phase shifts, waveform differences).
- The precise transfer function of the R1 sensor is not known. This leads to uncertainties in phase and amplitude information.

We are currently performing a number of laboratory tests using a step table developed by and in cooperation with Prof. Wielandt (retired from the University of Stuttgart, the father of broadband seismology). The goal is to determine the transfer function and to investigate the sensitivity of R1 to translations (and cross-axis-sensitivity).

### *d. Direct vs. array measurements of rotations*

Ground rotations are functions of the space derivatives of the seismic wavefield components through

$$\frac{1}{2}\nabla \times u = \frac{1}{2}\begin{pmatrix} \partial_y u_z - \partial_z u_y \\ \partial_z u_x - \partial_x u_z \\ \partial_x u_y - \partial_y u_x \end{pmatrix} \qquad (11)$$

This implies that – in principle - rotational ground motions can be derived by arrays of translation sensors by finite-differencing. Spudich et al. (1995) introduced the “seismogeodetic method” through which the components of rotations are derived from a surface seismic array. The explicit assumption of this method is that the strain tensor (in other words, the wavefield gradient) is spatially uniform over the extent of the array. To guarantee this, **one low-pass filters the ground motion data to remove signals with seismic wavelengths, measured along the direction(s) of interest, shorter than 4*h*, where *h* is the corresponding extent**

**of the array**. The factor of four is derived in Spudich and Fletcher (2008, pdf attached). This technique was applied several times to derive ground rotations (e.g., Huang, 2003, Spudich et al., 1995, 2008). However, the first time that array-derived ground rotations were compared with direct measurements of rotations (vertical axis) was reported by Suryanto et al. (2006). Later (Wassermann et al., 2009, see Figure 2) compared array-derived rotations for all three components with recordings using the R1 sensor described above.

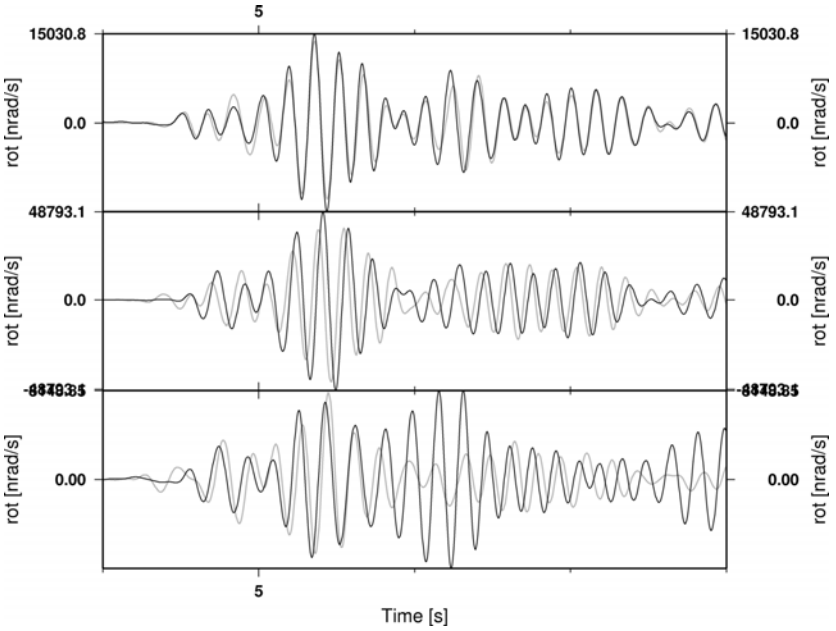


**Figure 2.** Direct comparison between R1 (black) and array-derived rotation (gray).Top: z-component; Middle: N-component; Bottom: E-component. Note the excellent waveform similarity for the z-component and the mismatch for the other components. (From Wassermann et al., 2009).

Suryanto et al. (2006) reported excellent agreement between array-derived and directly measured rotations (vertical component only) for broadband seismic measurements and a seismic array with a diameter of approximately 3km. The results by Wassermann et al. (2009) indicate good agreement in rotation rate (peak) amplitudes in the considered frequency band but only for the vertical component of rotation rate a good waveform match could be observed. It is important to note that – as studied in detail by Suryanto et al. (2006) – array derived rotations are sensitive to amplitude uncertainties and phase errors in the seismic data. **Therefore, it is recommended to use extremely well calibrated motion sensors (preferable of the same type) to perform array-estimates of rotations (or strain).**

The minimum number of stations needed to derive constant wave-field gradients is three. In both experimental studies comparing array-derived and directly measured rotations (with up to 9 stations) we find that the waveform fit depends substantially on the number and quality of stations used. This indicates that either non-constant wavefield gradients, difference in instrument response, noise, coupling, etc. are present in the array recordings. Suryanto et al. (2006) investigated such effects using synthetic seismograms. In the case of the 3 km array and broadband recordings we observed that using all nine array stations led to the best fit with directly measured rotations (Suryanto et al., 2006). This indicates that uncorrelated noise plays a role and averages out the more stations are used to derive rotations. **Therefore, we conclude that an optimal receiver configuration and an optimal number of receivers strongly depends on the quality of the individual recording sites and the uniformity of the instrument responses.**

## 3. Co-processing of rotations and translations

One of the key questions is, how joint measurements of rotations and translations can be used to improve solving seismic inverse problems. So far we have concentrated on the structural imaging. However, it is likely that rotations also improve the recovery of seismic source properties. Most developments described below are based on a simple plane wave analysis

that shows the tight link between transverse acceleration (or velocity) and rotation rate (or rotation angle).

Let us assume a transversely polarized plane wave with displacement $\mathbf{u} = (0, u_y(t - x/c), 0)$ , c being the horizontal phase velocity. The vector of rotation (curl) is thus given as

$$\Omega = \frac{1}{2}\nabla \times \dot{\mathbf{u}} = (0,0,-\frac{1}{2c}\ddot{u}_y(t - x/c)) \qquad (12)$$

This implies that – under the given assumptions – at any time rotation rate and transverse acceleration are in phase and the amplitudes are related by $\ddot{u}_y(x,t)/\Omega_z(x,t) = -2c$ . In the following we show with some examples the consistency of broadband ring laser recordings with this prediction.

### *a. Phase velocities*

To recover (apparent) phase velocities in a seismic wavefield usually requires observations from a seismic array and array processing tools. From equation (12) we can see that accurate observations at the same location of transverse accelerations and rotation rate should allow the estimation of phase velocities. This has first been demonstrated in Igel et al. (2005) and tested against synthetic seismograms calculated for a 3-D Earth model (see Figure 3).

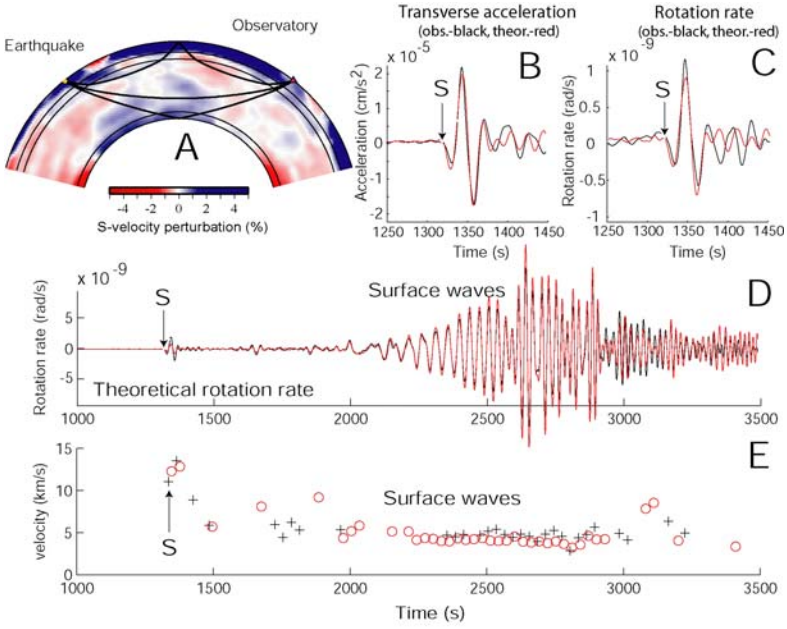


**Figure 3** Modelling of rotational ground motions, comparison with observations. The cut-off period is 20 s. **A**, Schematic view of some ray paths (S, ScS, SS) in a cross section through a 3-D global velocity model. **B**, Observed (black) and theoretical (red) transverse acceleration of the direct S-wave. **C**, Observed (black) and theoretical (red) rotation rate of the direct S-wave. **D**, Theoretical rotation rate (red) and converted rotation rate from theoretical transverse accelerations (black). **E**, Superposition of estimated horizontal phase velocities from observations (black crosses) and theory (red circles). (From Igel et al. 2005).

The results illustrate convincingly that phase velocities can be estimated from collocated recordings of translation and rotations. The most promising application of this for regional wave propagation is the estimation of Love-wave dispersion curves. As reported by Igel et al. (2007), time-domain estimates of the phase velocities in windows containing Love waves lead to frequency-dependent phase velocities. This analysis can in principle also be carried out in the frequency domain as suggested by Ferreira and Igel (2009): the Love-wave dispersion curves naturally drops out from the ratio of theoretical transverse acceleration and rotation rate in the generalized ray-theory formulation. The question, which spatial volume is responsible for the observed Love-wave dispersion estimates led to the application of the adjoint method to this problem as it allows the calculation of sensitivity kernels (see below).

### b. *Propagation directions*

As indicated by equation (12) transverse acceleration and rotation rate (around a vertical axis) should be in phase (i.e., have the same waveform, assuming linear superposition of waves propagating in the same direction). This indicates that waveform comparison (using cross-correlation techniques) should be the right tool to test this assumption. **In addition, if the direction of (shear-type) waves is not known, one can use cross-correlation techniques to estimate this direction. This might be interesting in particular when linear arrays (e.g., borehole receiver strings) are used and obtaining constraints on the azimuth of the propagating energy is difficult.** The principle is illustrated in Figure 4 (from Igel et al., 2007). Basically one rotates the horizontal sensors in any transverse direction and calculates the zero-lag cross-correlation coefficients in time windows of appropriate length (usually on the order of twice the dominant period). We expect that the correlation between assumed transverse acceleration and rotation rate is best in when the correct transverse direction is found. We find that direction of propagation (back-azimuths) can be estimated to within a few degrees. This processing is applied to the synthetic data in Part II of this report.

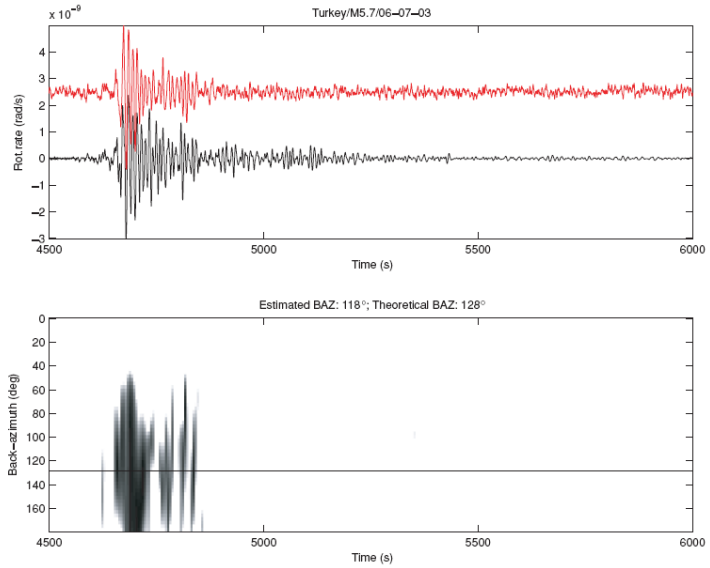


**Figure 4.** Top: Rotation rate and transverse acceleration (scaled to rotation rate) for the Turkey event, M5.7, 2003 July 6. Bottom: Zero-lag normalized correlation coefficient in a 20 s sliding time window between rotation rate and transverse acceleration, varying the unknown transverse direction from 0◦ to 180◦ (defined between 0.9-white and 1.0 black). The theoretical backazimuth is indicated by a horizontal line (see text for details). Summing up over time leads to a maximum in the direction of propagation (e.g., Pham et al., 2009, see also part II).

### c. *Scattering properties*

The partitioning of P and S energy and the stabilization of the ratio between the two is an important constraint on the scattering properties of the medium. It was a surprise to discover considerable rotational energy in a time window containing the P-coda (Igel et al., 2007). The ring laser – recording motions around a vertical axis only – should be sensitive to SH-type motion only. Other causes (e.g., tilt-ring laser coupling, topography, anisotropy) are estimated to be small.

An example of P-coda rotations is shown in Figure 5. Rotational motions above noise level can be seen right after the onset of the P-wave. When calculating the correlation between translation and rotations for all observed events (even then the P-Coda rotation is hidden in the noise) the correlation increases. This is a strong indication that correlated SH-type motions are picked up by the rotation sensor. This was extensively investigated by Pham et al. (2009). The most likely cause of this new type of observation was P-SH scattering close to the receiver location. Observational support for this hypothesis came from azimuth-dependent correlation coefficients calculated in different frequency bands (Figure 5, bottom traces). At low frequencies correlation is high in the direction of the theoretical backazimuth. At high frequencies correlation is high an almost all directions in the P-coda time window. This indicates that SH-type energy is coming from all directions indicative of scattering medium.

This was further tested simulating plane P-wave propagation through 3-D random media. From the observations the ratio between peak vertical ground velocity and rotation rate could be extracted and modelled with synthetic seismograms (Figure 6). It turned out that a crustal medium with 5-6% velocity perturbation at a correlation length of 5 km (not well constrained) can explain the observed ratios. **This indicates that – if rotational motions are available – the ratio between translational and rotational energy in appropriate time windows can help putting constraints on the average scattering properties of the medium.** As in the case of phase velocity estimates these constraints would correspond to structures close to the receiver locations. In a borehole context it might be possible to constrain time-dependent changes of structure around the receivers (e.g., from fluid injection or extraction).

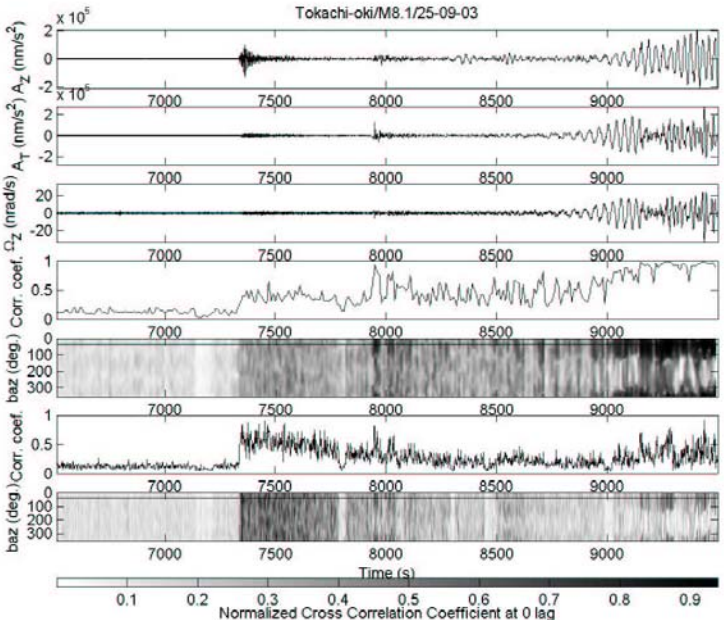


**Figure 5.** Top three traces: Vertical, transverse accelerations and rotation rate, respectively, for the Tokachi-oki event 25-09-2003, M8.1. The fourth and sixth traces (from top): zero lag normalized cross-correlation coefficients between rotation rate and transverse acceleration after high-pass filtering with cut-off periods 5s and 1s, calculated for 10s and 2s sliding time windows (respectively). The fifth and bottom: the correlation coefficients as a function of time and assumed back-azimuth (high pass filter with cut off period 5s and 1s, sliding time windows of 10s and 2s were applied respectively). The theoretical back-azimuth is indicated by a horizontal line.

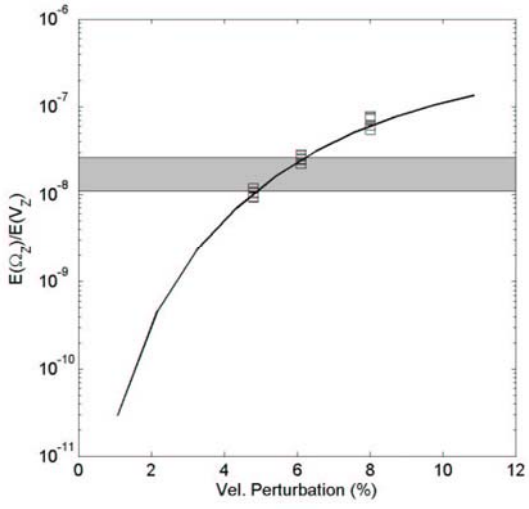


**Figure 6.** Comparison of observed and simulated energy ratios (vertical component of rotation rate to vertical component of ground velocity for P-waves propagating upwards). Black curve: the (average) energy ratio as a function of velocity perturbation calculated from simulated seismograms (correlation length fixed at 2000m); Squares: the (average) energy ratio as a function of correlation length (from 1000m up to 15000m) obtained from simulations; Horizontal gray band: range of the energy ratios obtained from observations.

## 4. The structural inverse problem with rotations

The simple relationship between transverse acceleration and rotation rate in the appropriate direction (as well as similar relationships between velocity and strain) and the possibility to derive “phase velocities” leads to an important question: what area (volume) is this measurement sensitive to? There are two options to investigate this: (1) calculating synthetic

data for various perturbations around a reference model and quantifying the effects on the data; or (2) solving the problem analytically using adjoint techniques. In the following we briefly describe the first application of the adjoint technique to this question (Fichtner and Igel, 2009) and the successful application to a new type of tomographic inverse problem (Bernauer, 2009; Bernauer et al., 2009). We restrict ourselves to a qualitative description here. Details can be found in the attached (p)reprints.

### *a. Adjoint method for "apparent shear wave speed": sensitivity kernels*

As mentioned above the ratio between ground acceleration (or velocity) and rotation rate (or rotation angle) has the dimension of a velocity. Only under very specific circumstances (e.g. relating the rotation around a vertical axis to transverse horizontal acceleration for S-waves propagating in horizontal direction in homogeneous media) this corresponds to the actual physical shear-wave speed. In general this ratio can be considered an "apparent shear-wave speed" and this is the observable we define to formulate the seismic inverse problem.

The "apparent shear-wave speed" $\beta_\alpha$ is defined as

$$\beta_\alpha = \frac{\left\| v(x^r) \right\|_2}{\left\| \omega(x^r) \right\|_2} \qquad (13).$$

$\beta_\alpha$ is the ratio of the rms displacement velocity measured at $x^r$ and the rms rotation amplitude $\omega$ measured at the same location $x^r$. The measurement is taken – using the $L_2$-norm - for a specific phase or waveform (the choice of an appropriate time window is important). Immediately some interesting properties can be derived: (1) No travel times need to be measured to determine $\beta_\alpha$. (2) For body waves in an unbounded and homogeneous medium $\beta_\alpha$ is equal to the true S-wave speed. This suggests that $\beta_\alpha$ contains directly observable information about Earth structure; (3) The apparent shear wave speed is independent of both the source timing and the source magnitude – two parameters that are often not well constrained.

Fichtner and Igel (2009) formulated the adjoint problem for this observable quantity and calculated sensitivity kernels for (1) the rms velocity measurements, (2) the rotation measurements; and (3) the ratio of both – the apparent shear-wave speed. Examples are shown in Figure 8 using ray theory to solve the forward problem. The sensitivity kernels show some characteristics that are highly relevant for the structural inverse problem:

- The size of the sensitivity kernels is frequency dependent, lower frequencies lead to broader kernels
- The individual kernels for velocity and rotation amplitudes look very similar to the well-known "banana-doughnut" kernels known from travel time problems
- For the "apparent shear-wave speed" kernels the sensitivity w.r.t. structure close to the source (except the singularity leading to sensitivity right at the source location) vanishes. This implies that $\beta_\alpha$ is primarily sensitive to structure in the vicinity of the receivers suggesting the possibility to formulate the inverse problem for structures close to the receivers

The kernels thus allow a precise quantification of the area to which the observed ratio is sensitive to. In principle this is possible for any background medium, if complete 3-D simulation technology is employed. In the next chapter a tomographic inversion scheme is proposed with which seismic inverse problems can be solved without the use of travel times!

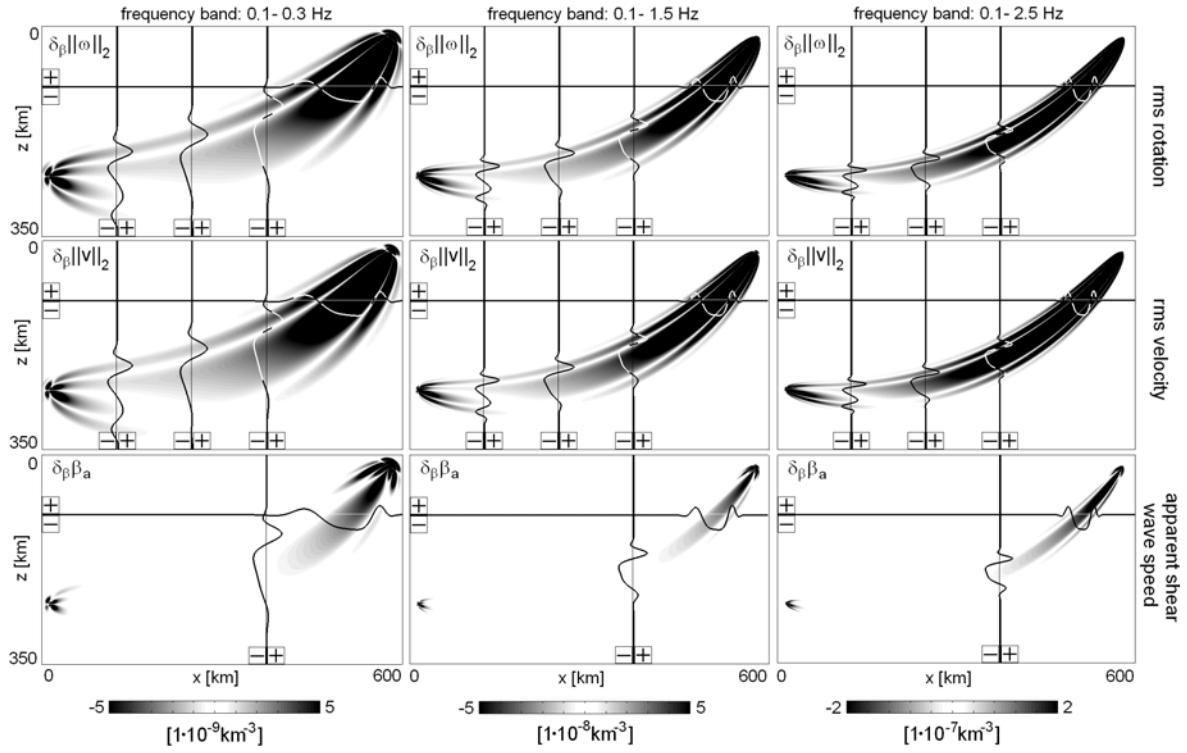


**Figure 8.** Sensitivity kernels for the rms rotation, $||\omega||_2$ (top row), the rms velocity, $||v||_2$ (middle row) and the apparent shear wave speed, $\beta_\alpha$ (bottom row). The columns correspond to different frequency bandwidths of the recorded velocity waveform: 0 − 0.3 Hz (left), 0 − 1.5 Hz (middle) and 0 − 2.5 Hz (right). Superimposed curves are normalised cuts through the sensitivity kernels in horizontal and vertical directions. All sensitivities are with respect to the S wave speed. The source is at 250 km depth and the receiver is near the surface.

### *b. Tomography with rotations – tomography without travel times*

The initial results by Fichtner and Igel (2009) raised expectations that the seismic inverse problem for Earth structure could be posed by fitting measurements of "apparent shear-wave speed" $\beta_\alpha$. To make the problem more tractable the rotation and velocity amplitudes (and the corresponding sensitivity kernels) for a given Earth model are calculated using ray theory. The seismic inverse problem can be formulated in an iterative way. The gradient of the misfit function comparing "observations" and "theoretical data" is obtained by superimposing the sensitivity kernels for each source receiver pair. It is important to note that such an inversion scheme rests entirely on the observation of (rms-) amplitudes in certain time windows and no travel time information is used. Nevertheless the model parameters that are recovered are physical (shear-) wave velocities. This shall be illustrated with a simple cross-hole synthetic example (Figure 9, for details please refer to Bernauer, 2009, and Bernauer et al., 2009).

The model contains two 80 m deep boreholes (vertical white columns) at 80m distance. Sources and receivers are equally spaced between 5 and 75 m depth. The receiving borehole contains 70 sensors recording the signals (rotation and velocity amplitudes) from eight sources in the borehole. The synthetic model contains low- and high-speed variations on a constant S velocity background of 2 km/s. The model is described using a set of basis functions (cubic blocks).

The inversion starts with a misfit minimisation for a homogeneous initial model and the smallest frequency band (here 0.1 - 0.6 kHz). After seven iterations the synthetics reproduce the observations well, and the resulting image can be used as initial model for the inversion in the next higher frequency band. We repeat this procedure until we find satisfactory fit with the

observations. The final model is presented in the right panel of figure 9. The inversion result localises low- and high-velocity zones correctly. The shapes and the intensities of the perturbations are similar to the original model. Small differences in the shape of the perturbations remain. They may be attributed to an imperfect data coverage. We note that this example is a proof of concept and not a systematic resolution study that would need to be performed for each specific application.

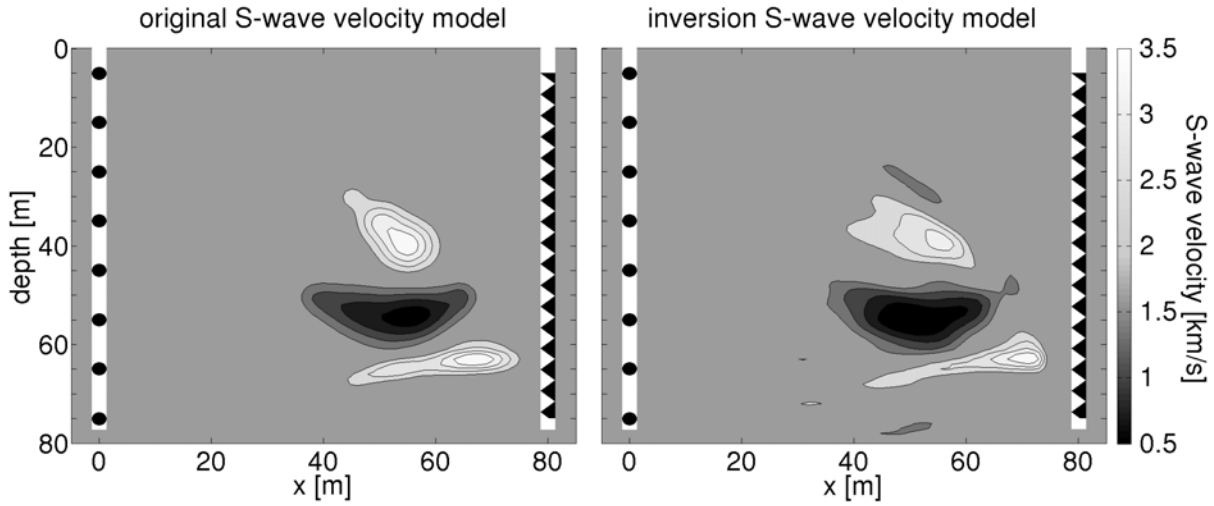


**Figure 9.** Left: Crosshole tomography scenario with two 80 m deep boreholes (vertical white columns) at 80m distance. Sources and receivers are equally spaced between 5 and 75 m depth. The right borehole contains 70 receivers (black sawtooth line) recording the signals from eight sources (black bullets) in the left borehole. The synthetic model contains low- and high-speed variations on a constant S velocity background of 2 km/s. Right: Final model after inversion in the successively broader frequency bands. The original model on the left is well reproduced.

Even though these results are promising and suggest new ways of solving the seismic inverse problems substantial further research is necessary to (1) understand the behaviour of such a tomographic scheme for a wide range of velocity perturbation amplitudes and spatial scales; (2) quantify uncertainties particularly in the presence of errors in the amplitude measurements; and (3) study the scheme for various source-receiver geometries.

## 5. Conclusions and recommendations

In this report we presented recent progress in the area of theory, observations, and processing (inversion) of rotational ground motions and illustrate potential applications in oilfield studies. In this section we summarize these results and formulate some recommendations for specific applications and further studies. These will be complemented by part II of the report with processing of synthetic 6-component seismograms for the source-receiver setup suggested by SLB.

The key results and recommendations are:

- Except for measurements close to (large) seismic sources high-resolution rotation sensors are necessary. For microseismicity studies in oilfield applications we estimate that rotational motions should be detectable at least down to approx. $10^{-7}$ rad/s. To the best of our knowledge there is currently no borehole sensor satisfying these constraints. The only commercial surface rotation sensor for seismics (R1 from eentec) is capable of measuring motions in this amplitude range. However, questions remain on the applicable frequency range and the precise transfer function of this sensor.

- The (additional) measurement of rotational ground motions allow (in isotropic media) the separation of P- and S-energy. For complicated seismograms this might facilitate the identification of shear phases.

- In anisotropic media no pure shear or compressional wave exists and the P-wave has a non-zero curl contribution. This effect is currently being quantified and it might be possible to use this effect to constrain anisotropic properties in the vicinity of the receiver.

- The ratio of translational and rotational motions allows the recovery of wavefield information that is otherwise only accessible through array measurements. This holds in particular for the determination of (apparent) shear- or Love-type phase velocities. As these phase velocities are sensitive to the Earth's elastic properties, the collocated measurements of rotations and translations can be used to solve the seismic inverse problem for structure.

- An observable can be defined ("apparent shear-wave speed") that is the ratio of rms ground velocities and rotations. An inverse problem for Earth structure (shear wave velocities) can be formulated using adjoint techniques. Initial synthetic tests show that shear-wave structure can be recovered inverting observations of "apparent shear-wave speed". It is important to note that no travel time information is required in the process.

- Under the assumption of plane-wave propagation (and appropriate vectorial orientation) the waveforms of translations and rotations are identical. This can be quantified using cross-correlation techniques. This property can be exploited to determine the direction of shear-wave propagation (i.e., backazimuth) by maximising the zero-lag cross-correlation coefficient as a function of propagation direction. This might be interesting particularly when linear seismic arrays are being used and backazimuths are not well constrained from translation measurements alone.

- Observations of rotational energy prior to the onset of the direct shear wave indicates P-S converted energy in the vicinity of the receiver. The ratio of rotational to translational energy allows putting constraints on the scattering property of the medium around the receiver. It is conceivable that temporal changes (e.g., through fluid migration, changes of pore-space content) might be detectable.

- In two cases of very different scale (3km, 50m) we find good agreement between array-derived rotations and directly measured rotations. However, it is important to note that array-derived rotations are sensitive to local short scale structural heterogeneities, errors in amplitude (instrumental, coupling, transfer function, etc.) that are often hard to quantify.

## References

(bold articles are attached as pdf re/pre-prints)


Aki, K. & Richards, P. G. *Quantitative Seismology*, 2nd Edition, University Science Books (2002).

**Bernauer, M., Fichtner, A., Igel, H., Inferring near-receiver structure from combined measurements of rotational and translational ground motions, Geophysics, submitted (2009).**

**Bernauer, M., Tomography with rotations, Diploma Thesis LMU Munich, 2009.**

**Cochard, A., Igel, H., Schuberth, B., Suryanto, W., Velikoseltsev, A., Schreiber, U., Wassermann, J., Scherbaum, F., Vollmer, D. Rotational motions in seismology: theory, observations,**

**simulation, in "*Earthquake source asymmetry, structural media and rotation effects*" eds. Teisseyre et al., Springer Verlag (2006).**

**Ferreira, A., Igel, H., Rotational motions of seismic surface waves in a laterally heterogeneous Earth, *Bull. Seism. Soc. Amer.*, in print, (2009).**

**Fichtner A. and Igel H., Sensitivity densities for rotational ground motion measurements, *Bull. Seism. Soc. Amer.*, in print, (2009).**

Graizer, V. M. Effect of tilt on strong motion data processing, Soil Dyn. Earthq. Eng, 25, 197-204 (2005).

Graizer, V. M. Equation of pendulum motion including rotations and its implications to the strong-ground motion, in Earthquake Source Asymmetry, Structural Media and Rotation Effects, 471-491 (2006).

Huang, B. S. (2003). Ground rotational motions of the 1999 Chi-Chi, Taiwan, earthquake as inferred from dense array observations, *Geophys. Res. Lett.* **30,** 1307–1310.

**Igel, H., Cochard, A., Wassermann, J., Flaws, A., Schreiber, U., Velikoseltsev, A., Pham, D.N. Broadband Observations of Earthquake Induced Rotational Ground Motions, *Geophys. J. Int.*, 168, 182-196, doi: 10.1111/j.1365-246X.2006.03146x, (2007).**

**Igel, H., Schreiber, K.U., Flaws, A., Schuberth, B., Velikoseltsev, A., Cochard, A., Rotational motions induced by the M8.1 Tokachi-oki earthquake, September 25, 2003, *Geophys. Res. Lett.*, 32, L08309, doi:10.1029/2004GL022336 (2005).**

Lee et al. (2009), Progress in Rotational Ground-Motion Observations from Explosions and Local Earthquakes in Taiwan, Bull.Seis.Soc.Amer., in print.

Lin, C.J., et al., Recording Rotational and Translational Ground Motions of Two TAIGER Explosions in Northeastern Taiwan on 4 March 2008, Bull.Seis.Soc.Amer., in print**.**

Liu, C.C. et al., Observing Rotational and Translational Ground Motions at the HGSD Station in Taiwan from 2007 to 2008, Bull.Seis.Soc.Amer., in print**.**

McLeod, D.P., Stedman, G.E., Webb, T.H. & Schreiber, U. Comparison of standard and ring laser rotational seismograms. *Bull. Seism. Soc. Amer.* 88, 1495-1503 (1998).

Nigbor et al., Laboratory and Field Testing of Commercial Rotational, *Bull. Seism. Soc. Amer.*, in print, (2009).

Pancha, A., Webb, T.H., Stedman, G.E., McLeod, D.P. & Schreiber, U. Ring laser detection of rotations from teleseismic waves. *Geophys. Res. Lett*. 27, 3553-3556 (2000).

**Pham D.N., Igel H., Wassermann, J., M. Käser, J. de la Puente, Schreiber, U. Observations and modelling of rotational signals in the P-Coda: constraints on crustal scattering, *Bull. Seism. Soc. Amer.*, in print, (2009).**

**Pham, D.N., Igel H., Wassermann, J., Schreiber, U., A. Cochard, The effects of tilt on interferometric rotation sensors, *Bull. Seism. Soc. Amer.*, submitted, (2009).**

**Schreiber, U., J. N. Hautmann, A. Velikoseltsev, J. Wassermann, H. Igel, J. Otero, F. Vernon, and J.-P. R. Wells, Ring Laser Measurements of Ground Rotations for Seismology, Bull. Seis. Amer. Soc., in print (2009).**

Schreiber, U., Stedman, G.E., Igel, H., Flaws, A. Ring laser gyroscopes as rotation sensors for seismic wave studies. In "*Earthquake source asymmetry, structural media and rotation effects*" eds. Teisseyre et al., Springer Verlag (2006).

Spudich, P, and J. B. Fletcher, (2008). Observation and prediction of dynamic ground strains, tilts, and torsions caused by the M6.0 2004 Parkfield, California, earthquake and aftershocks derived from UPSAR array observations, Bull.Seis.Soc.Amer., accept. for publication.

Spudich, P., L. K. Steck, M. Hellweg, J. B. Fletcher, and L. M. Baker (1995). Transient stresses at Parkfield, California, produced by the M7.4 Landers earthquake of June 28, 1992: Observations from the UPSAR dense seismograph array, *J. Geophys. Res.* **100,** 675–690.

**Suryanto, W., J. Wassermann, H. Igel, A. Cochard, D. Vollmer, F. Scherbaum, A. Velikoseltsev, and U. Schreiber (2006), First comparison of seismic array derived rotations with direct ring laser measurements of rotational ground motion, Bull. Seism. Soc. Am., 96(6), 2059-2071, doi:10.1785/0120060004.**

**Suryanto, W. (2006): Rotational Motions in Seismology: Theory and Application. Dissertation, LMU München: Fakultät für Geowissenschaften**

Trifunac, M.D. & Todorovska, M.I. A note on the usable dynamic range of accelerographs recording translation. *Soil Dyn. and Earth. Eng*. 21(4), 275-286 (2001).

**Wassermann, J., S. Lehndorfer, H. Igel, U. Schreiber (2009), Performance test of a commercial rotational motion sensor, Bull.Seis.Soc.Amer., in print.**

# Appendix A: Peak translations and rotations

Complete set of figures for peak ground motions described in section 2a.

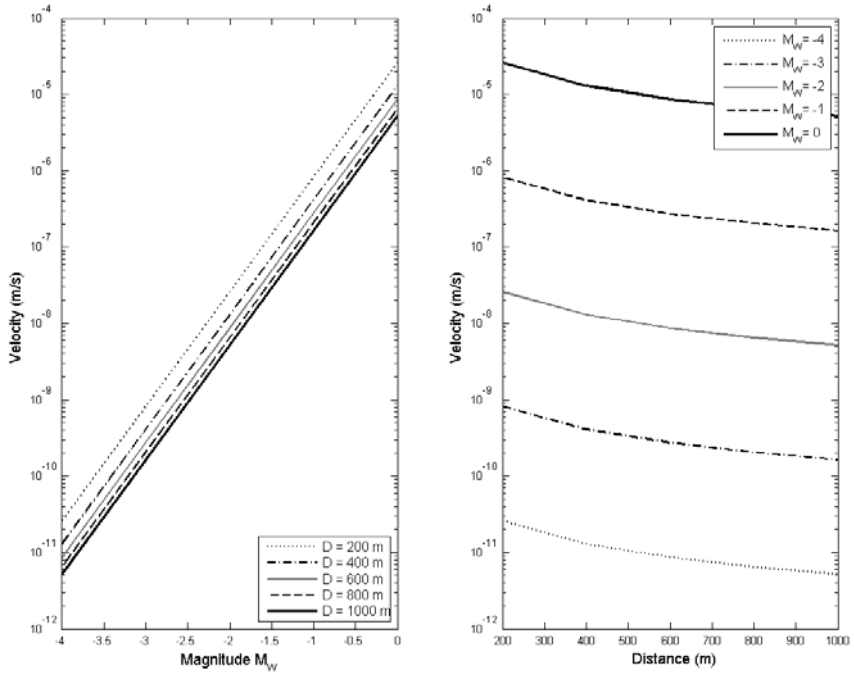


**Figure A1.** Peak translational velocity predicted for a dominant frequency *f* = 15 Hz as a function of magnitude and hypocentral distance.

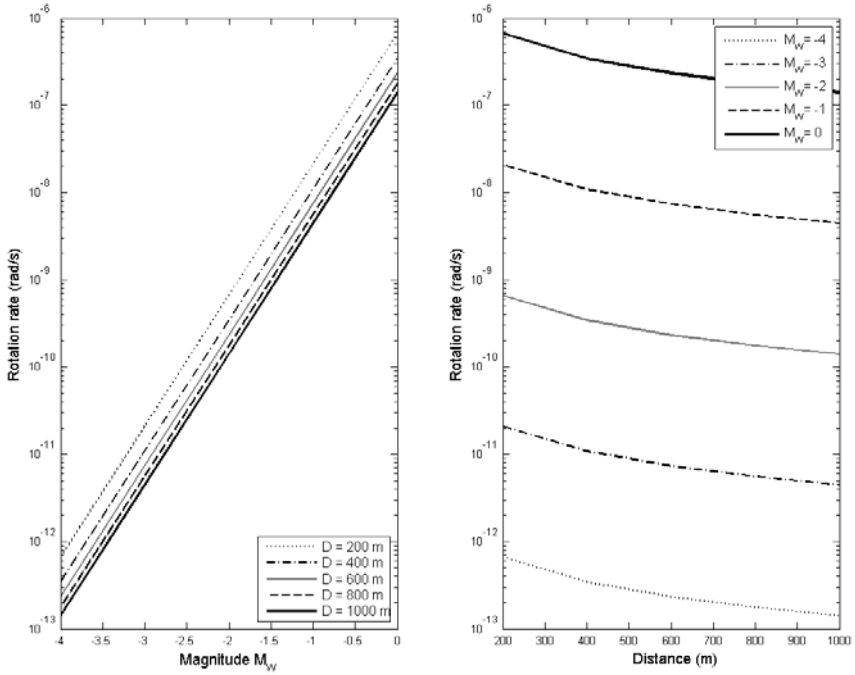


**Figure A2.** Peak rotation rate predicted for a dominant frequency *f* = 15 Hz as a function of magnitude and hypocentral distance.

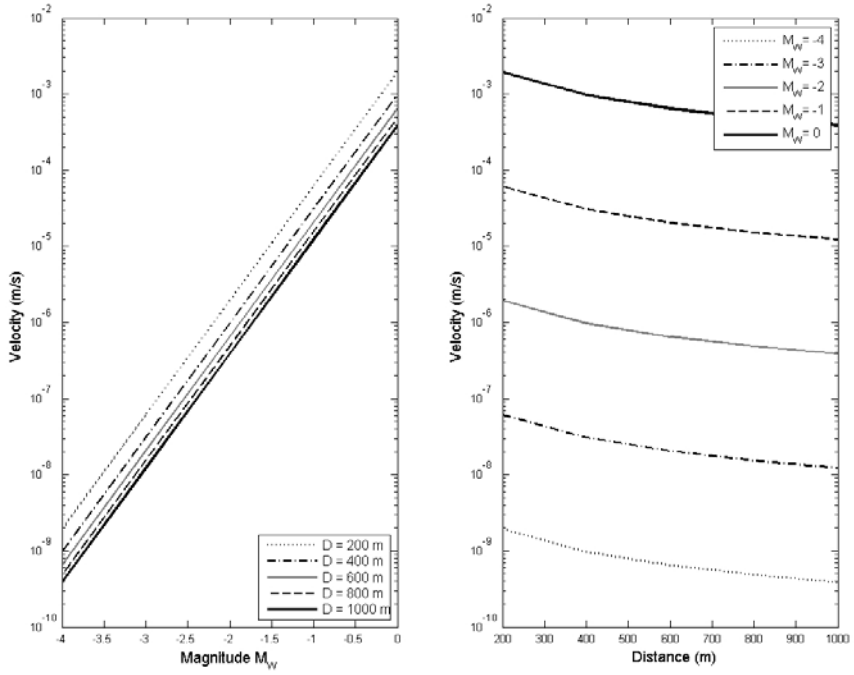


**Figure A3**. Peak translational velocity predicted for a dominant frequency *f* = 150 Hz as a function of magnitude and hypocentral distance.

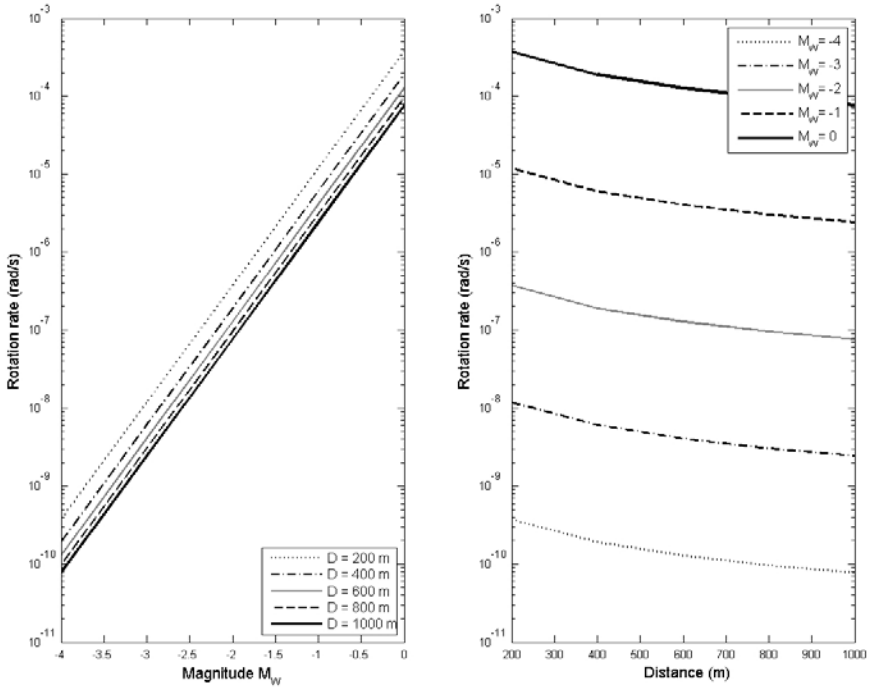


**Figure A4.** Peak rotation rate predicted for a dominant frequency *f* = 150 Hz as a function of magnitude and hypocentral distance.